



Changes of olfactory tract in Parkinson's disease: a DTI tractography study

Pasquale Nigro¹ · Andrea Chiappiniello² · Simone Simoni¹ · Federico Paolini Paoletti¹ · Giulia Cappelletti¹ · Pietro Chiarini³ · Marta Filidei¹ · Paolo Eusebi⁴ · Giorgio Guercini³ · Valerio Santangelo^{5,6} · Roberto Tarducci² · Paolo Calabresi^{7,8} · Lucilla Parnetti⁴ · Nicola Tambasco^{1,4}

Received: 20 May 2020 / Accepted: 7 September 2020 / Published online: 11 September 2020

© Springer-Verlag GmbH Germany, part of Springer Nature 2020

ABSTRACT

Purpose Impaired olfactory function is one of the main features of Parkinson's disease. However, how peripheral olfactory structures are involved remains unclear. Using diffusion tensor imaging fiber tracking, we investigated for MRI microstructural changes in the parkinsonian peripheral olfactory system and particularly the olfactory tract, in order to seek a better understanding of the structural alternations underlying hyposmia in Parkinson's disease.

Methods All patients were assessed utilizing by the Italian Olfactory Identification Test for olfactory function and the Unified Parkinson's Disease Rating Scale-III part as well as Hoehn and Yahr rating scale for motor disability. Imaging was performed on a 3 T Clinical MR scanner. MRI data pre-processing was carried out by DTIPrep, diffusion tensor imaging reconstruction, and fiber tracking using Diffusion Toolkit and tractography analysis by TrackVis. The following parameters were used for groupwise comparison: fractional anisotropy, mean diffusivity, radial diffusivity, axial diffusivity, and tract volume.

Results Overall 23 patients with Parkinson's disease (mean age 63.6 ± 9.3 years, UPDRS-III 24.5 ± 12.3 , H&Y 1.9 ± 0.5) and 18 controls (mean age 56.3 ± 13.7 years) were recruited. All patients had been diagnosed hyposmic. Diffusion tensor imaging analysis of the olfactory tract showed significant fractional anisotropy, and tract volume decreases for the Parkinson's disease group compared with controls ($P < 0.05$). Fractional anisotropy and age, in the control group, were significant for multiple correlations ($r = -0.36$, $P < 0.05$, Spearman's rank correlation).

Conclusions Fiber tracking diffusion tensor imaging analysis of olfactory tract was feasible, and it could be helpful for characterizing hyposmia in Parkinson's disease.

Keywords Parkinson's disease · MRI · Magnetic resonance · Smell · Olfactory function

Introduction

Parkinson's disease (PD) is a multisystem disorder, and it is widely accepted that motor features are preceded by a

prodromal “pre-motor” phase, including a wide range of non-motor symptoms (NMS) [1]. The basis for these NMS is that the pathologic process may not start in the substantia nigra pars compacta. According to the “dual hit hypothesis,” a

✉ Nicola Tambasco
n.tambasco@libero.it

¹ Movement Disorders Center, Neurology Department, Perugia General Hospital and University of Perugia, S. Maria della Misericordia Hospital, Perugia, Italy

² Department of Medical Physics, Perugia General Hospital, Perugia, Italy

³ Neuroradiology Unit, Perugia General Hospital, Perugia, Italy

⁴ Neurology Department, Perugia General Hospital and University of Perugia, Perugia, Italy

⁵ Department of Philosophy, Social Sciences & Education, University of Perugia, Perugia, Italy

⁶ Neuroimaging Laboratory, IRCCS Santa Lucia Foundation, Rome, Italy

⁷ Neurologia, Fondazione Policlinico Universitario Agostino Gemelli IRCCS, Rome, Italy

⁸ Dipartimento di Neuroscienze, Università Cattolica del Sacro Cuore, Rome, Italy

neurotropic pathogen could enter the brain via two routes, nasal and/or gastric pathways, progressively reaching the central nervous system [2]. Neuropathological works in PD revealed that specific brain pathology extends far beyond the nigrostriatal dopaminergic system and affects widespread brain areas [3].

Converging evidences suggest that 75–90% of patients with PD exhibit marked olfactory disturbances, and it is firmly established that loss of sense of smell precedes the development of motor symptoms by a decade or before [4]. Moreover, idiopathic olfactory impairment has a high predictive value in developing PD [5] with a relative risk estimated to be 3.9- to 5.2-fold in population-based studies [6].

The multiple components' pathophysiology of olfactory dysfunction in PD remains poorly understood: neuropathological studies have reported that the PD-related olfactory impairment seems not to be directly associated with specific changes in the olfactory epithelium [7], but with processes associated with Lewy body formation in several different areas of the olfactory system [8]. Postmortem studies have documented that the olfactory bulb is one of the earliest affected sites in PD pathology [9]. Nowadays, impaired olfactory function is recognized as one of the earliest indicators of developing PD and one of the major NMS, with a significant impact on quality of life [10]. The combination of imaging correlates for olfactory dysfunction with clinical measures could be useful to identify suspected pre-motor PD patients. The use of conventional MRI has so far been the differentiation of PD from symptomatic parkinsonism and from degenerative atypical parkinsonian disorders. Modern neuroimaging techniques have been widely applied to provide imaging pattern differentiating patients from age-matched HC [11].

To date, neuroimaging correlates of olfactory dysfunction in PD have been reported in few studies. Su and colleagues, in a resting-state functional MRI study, showed, in hyposmic PD patients, altered functional activity not only in parts of the traditional olfactory regions but also in some nontraditional olfactory centers of the limbic/paralimbic cortices [12]. Structural MRI studies also detected abnormalities in the cerebral olfactory system. In a diffusion-weighted imaging study, an increased diffusivity in the olfactory tract was found in early PD patients [13], and, in a diffusion tensor imaging (DTI) study, a correlation between diffusion indices in the cerebellum and odor recognition thresholds was reported [14]. Moreover, Ibarretxe-Bilbao and colleagues, using tract-based spatial statistics, demonstrated microstructural changes in the gyrus rectus and in the white matter surrounding primary olfactory areas of PD patients [15]. DTI is a non-invasive MRI technique, which provides information on the mobility of water molecules in the microenvironment [16]. In particular, the diffusion tensor describes the diffusion behavior along a range of directions [17]. Pathological processes of axonal damage and loss that modify the molecular environment affect

DTI parameters. Furthermore, DTI can be used to reconstruct axonal tracts (fiber tracking), including the large-scale structural connections of the brain [18]. DTI parameters have already been used in some pathologies as markers of structural damage [19]; neuronal loss and disruption within the bundle-like architecture of the olfactory-tract are prone to be depicted by DTI. The olfactory tracts are localized in the olfactory grooves, travelling posteriorly on the inferior surface of the frontal lobe. Distally the tracts reach the anterior perforated substance, and they split into medial, intermediate, and lateral striae. The olfactory tracts are anatomically close to air-filled sinuses and therefore exposed to susceptibility artifacts. The feasibility of fiber tracking DTI analysis of the olfactory tract has already been investigated in 5 healthy individuals and 1 PD patient by Skorpil and colleagues [20]. In all five healthy individuals examined, the olfactory tracts could be fiber tracked. In contrast, in the only anosmic patient examined olfactory tracts were not visualized.

The purpose of the present paper was to investigate for MRI microstructural changes in the parkinsonian peripheral olfactory system and particularly the olfactory tract, in order to seek a better understanding of the structural alternations underlying hyposmia in Parkinson's disease.

Subjects/materials and methods

Subjects

Twenty-three PD patients (15 male; overall age range 36–82; overall mean age 63.6 ± 9.3 years, mean disease duration 2.7 ± 2.3 years), fulfilling the established United Kingdom Parkinson's Disease Society Brain Bank Clinical Diagnostic Criteria [21], were recruited from the Movement Disorders Unit, Neurology Service, Hospital Clinic, in Perugia, while 18 healthy controls (HC), age-matched to patients (12 male; overall age range 33–84; overall mean age 56.3 ± 13.7 years), were recruited from volunteers including spouses and/or friends between 2015 and 2018. None of the control subjects had a history or signs of neurological disorders.

All subjects were assessed with a neurological exam. All patients received regular L-dopa therapy and/or dopamine agonists and were taking their recommended PD medication during the clinical assessment. Motor disability related to parkinsonism was assessed in all patients in ON drug states using part III of the Unified Parkinson's Disease Rating Scale (UPDRS III), and disease stages were classified according to the Hoehn and Yahr rating scale (H&Y).

Exclusion criteria for all subjects included history of head trauma, previous maxilla-facial surgery, nasal fracture or diagnosis of rhinitis and/or nasal polyps, detection of expansive lesions in the anterior cranial fossa, and Mini-Mental State Exam (MMSE) score ≤ 24 .

Olfactory testing

Prior to MRI, olfactory function of each patient was assessed by means of the Italian Olfactory Identification Test (IOIT), which consists of 33 odorants familiar to Italy. This test has been utilized in Italy for primarily screening PD patients [22].

The procedure started with the administration of tester n°1, up until n°33. First the suggested answers for each tester were read, and then the tester was rubbed and sniffed (the smelling area of the tester was positioned not more 1 cm under the patient's nose). The patients had to choose one of the answers among the four suggested, crossing or circling it.

Based on the IOIT score, hyposmia was identified, according to the age, using the following cutoff: age range 30–49 → score > 4, age range 50–59 → score > 5, age range 60–69 → score > 6, and age range 70–79 → score > 7.

Patients were taking dopaminergic treatment at the time of olfactory function testing, since no modifying effect of levodopa was reported [23, 24].

MRI

MRI acquisition protocol

PD patients and controls were scanned with a 3 T Philips Achieva, using an 8-channel head coil. For the neuroradiological report, the MRI protocol included an anatomical FLAIR sequence (axial acquisition, FOV = 230 × 230 mm², pixel size = 0.45 × 0.45 mm², slice thickness = 4 mm, number of slices = 29 with a slice gap of 1 mm, TE = 125 ms, TR = 11000 ms, flip angle = 90 deg, no fat suppression, full k-space, no averages), an anatomical T1-weighted sequence (sagittal acquisition, FOV = 250 × 250 mm², pixel size = 1.04 × 1.04 mm², slice thickness = 0.6 mm, number of slices = 301 without slice gap, TE = 3.4 ms, TR = 7.4 ms, flip angle = 8 deg, no fat suppression, full k-space, no averages), and an anatomical T2 sequence (axial acquisition, FOV = 230 × 230 mm², pixel size = 0.45 × 0.45 mm², slice thickness = 4 mm, number of slices = 29 with a slice gap of 1 mm, TE = 80 ms, TR = 3000 ms, flip angle = 90 deg, SPIR fat suppression, full k-space, no averages).

Diffusion-weighted (DW) data were acquired using a single-shot, spin-echo, echo-planar imaging (EPI) sequence across 32 different non-collinear diffusion directions with a b-factor of 1000 s/mm², along with an initial non-diffusion-weighted volume (acquisition parallel to the ethmoidal plane, FOV = 184 × 184 mm², voxel size = 1.8 × 1.8 × 1.8 mm³, number of slices = 45 without slice gap, TE = 55 ms, TR = 9700 ms, flip angle = 90 deg, SPIR fat suppression, full k-space, 2 averaged acquisitions). The TE was kept short by using maximum gradient strength/slew rate, parallel imaging, and partial Fourier encoding, whereas the 2 acquisitions increase the signal-to-noise ratio in the averaged image but double the scanning time. To reduce the DTI acquisition time to

about 12 min, parallel imaging (SENSE 2) was used and we chose not to cover the whole brain, limiting the acquisition to an approximately 8 cm cranio-caudal thickness, focusing on the olfactory tracts so to reduce any geometric warping.

DTI data processing and analysis

Dicom data were converted to the nifti format using the free dcm2nii software (<http://www.mccauslandcenter.sc.edu/mricro/mricron/dcm2nii.html>, output format FSL/SPM8—4D NIFTI).

Pre-processing of DW images was performed with DTIPrep [25], which automatically corrects for eddy current distortions and head motion by removing low-quality directions and reorienting the b-matrix.

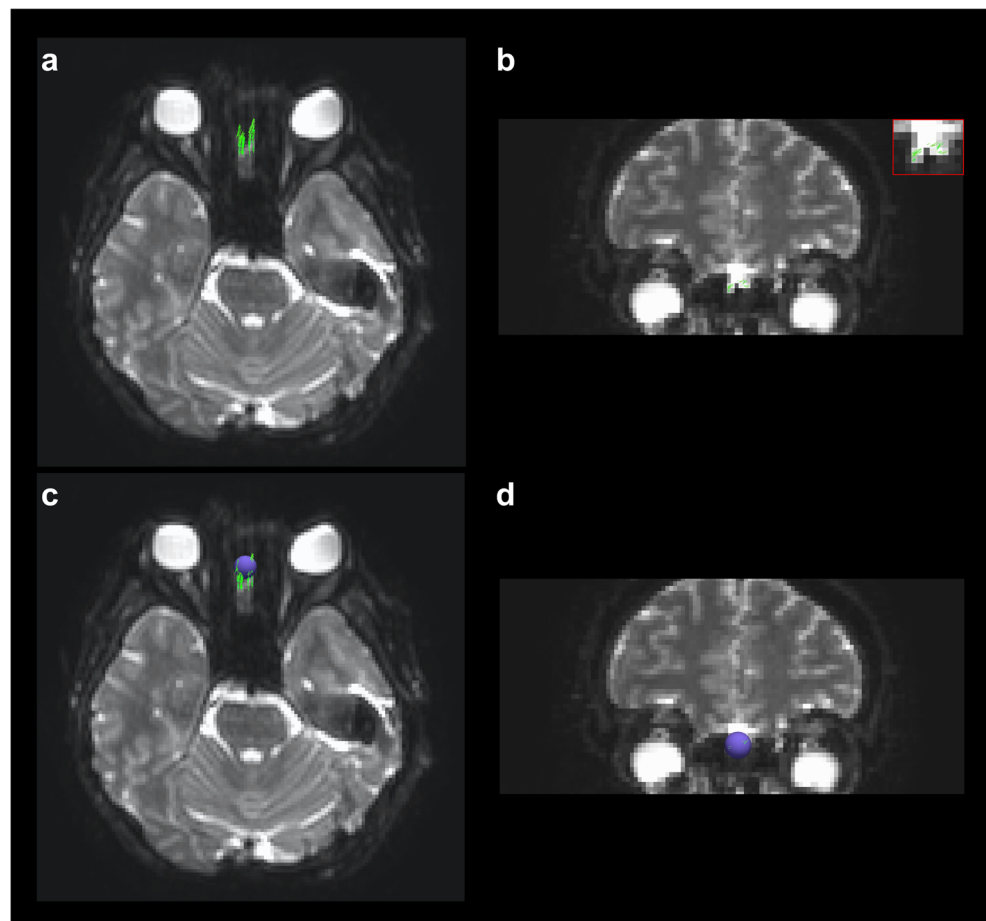
Afterwards, Diffusion Toolkit [26] was used both to estimate the diffusion tensors and to perform deterministic tractography utilizing the FACT propagation algorithm (angle threshold = 30 deg, minimum FA = 0.05, minimum track length = 1 mm) and applying a spline filter to clean up the tracks.

Virtual manual dissections of the olfactory tracts were performed, twice for each subject, with TrackVis [26] by a tractographer, who was blinded to the clinical status of each subject (PD patient/control) (Fig. 1a). A seed region of interest (ROI) was positioned in the olfactory tract distal region (including the olfactory bulbs), identified on a plane parallel to the ethmoidal plane (Fig. 1b), using the T2 images as an anatomical reference. Other ROIs were positioned to rule out spurious reconstruction artifact tracts of the visualized fibers. This was carried out by placing NOT-gated ROIs. Then, the estimates of the overall tract volume (TV), fractional anisotropy (FA), mean diffusivity (MD), radial diffusivity (RD), and axial diffusivity (AD) average values were automatically calculated by the software and registered for each subject. Finally, these estimates were averaged across the two dissections.

Statistical analysis

The statistical analysis was performed using R software v3.0. Descriptive statistics are reported here as means and standard deviations for continuous variables and absolute frequencies and percentages for categorical variables. The hypothesis of intra-rater agreement was substantiated for track volumes through intra-class correlation coefficient (ICC). Any differences between groups were tested utilizing ANCOVA for adjusting for the effect of age. The correlations between variables were calculated with Spearman's coefficients. Because the control cohort was overall significantly younger than PD group, we adjusted for this age difference when comparing tractography between the groups. For all analyses, a *P* value less or equal to 5% was considered statistically significant.

Fig. 1 Axial and coronal slices of the non-diffusion-weighted volume acquired along with the DW data where the olfactory bulb region is represented. (a–b) Virtual manual dissections of the olfactory tracts obtained on a control subject using TrackVis. (c–d) ROI placed in the olfactory bulb region for the dissection of the olfactory tracts (shown in purple)



Results

Clinical variables

Demographic information and clinical characteristics of the study population are listed in Table 1. The H&Y stages are identified as stage 1 in three patients, stage 1.5 in two, stage 2 in fourteen, stage 2.5 in three, and stage 3 only in one. The disease duration was 2.7 ± 2.3 years (range 1–10), while the median UPDRS III score was 24.5 ± 12.3 (range 9–53). The average IOIT score was 13.7 ± 4.9 (range 7–25).

Table 1 Subjects' characteristics (mean \pm SD)

| | PD patients ($n = 23$) | Controls ($n = 18$) |
|---------------------------|--------------------------|-----------------------|
| Male/female, no. | 15/8 | 12/6 |
| Age, year | 63.6 ± 9.3 | 56.3 ± 13.7 |
| Duration of disease, year | 2.7 ± 2.3 | |
| H&Y | 1.9 ± 0.5 | |
| UPDRS III | 24.5 ± 12.3 | |
| IOIT score | 13.7 ± 4.9 | |

Analysis of processed DTI data

ICC = 0.997 ($P < 0.001$) was found for track volumes provided by the two dissections for each subject, suggesting an almost perfect agreement. DTI analysis of the olfactory tract showed significant FA, and TV decreases for the PD group, when compared with the control group ($P < 0.05$) (Table 2, Fig. 2). No significant differences in MD/RD/AD between the two groups were observed. For only the HCs, but not PD group, a significant correlation was found between FA and age ($r = -0.36$, $P < 0.05$, Spearman's rank correlation) (Fig. 3).

Table 2 Results of the olfactory tract values (mean \pm SD)

| | Controls | PD patients | P |
|-------------------------|-----------------------|-----------------------|------------|
| FA | 0.159 ± 0.035 | 0.141 ± 0.002 | 0.028 |
| MD (mm ² /s) | 0.00140 ± 0.00020 | 0.00149 ± 0.00021 | 0.960 |
| AD (mm ² /s) | 0.0016 ± 0.0002 | 0.0017 ± 0.0003 | 0.640 |
| RD (mm ² /s) | 0.0013 ± 0.0002 | 0.0014 ± 0.0002 | 0.789 |
| TV (ml) | 0.982 ± 0.718 | 0.561 ± 0.287 | < 0.0001 |

FA fractional anisotropy, MD mean diffusivity, AD axial diffusivity, RD radial diffusivity, TV tract volume

Spearman's rank correlation coefficient revealed a trend for a positive correlation between RD and age ($r = 0.27$; $P = 0.08$). No significant correlations were found between FA/TV/MD/RD and parameters for motor function.

Discussion

In the present study, we tested olfactory function using IOIT, and the score of all PD patients was under the cutoff threshold. The DTI fiber tracking analysis detected structural differences of the olfactory tract between PD patients and HC, likely marks of neurodegenerative changes.

By applying a ROI-based approach focusing on the olfactory tract, previous studies have reported statistically significant regional signal changes in patients when compared with a group of HC. A recent meta-analysis [27] revealed that DTI is able to address structural differences between PD patients and HC particularly in olfactory tract. Two studies included in this meta-analysis have reported FA and MD changes between PD patients and HC

[24, 28]. Moreover, after examining the DTI-derived measures from 13 ROIs (non-motor brain regions implicated in early stages of PD according to Braak's hypothesis), Chen et al. found that FA values were lower in PD patients than HC in the olfactory tract [29]. Lastly, in DTI and statistical modeling report, the olfactory regions were particularly efficient at distinguishing de novo drug-naïve PD patients from HC [30].

Unlike previous studies, our study adopted fiber tracking to visualize the olfactory tracts. Specifically, while ROI-based techniques depend on *a priori* assumption of the size and shape of the region to be evaluated, without *a priori* hypothesis regarding the localization of the olfactory tract, tractography provides better accuracy. In order to minimize susceptibility artifacts [20], we used an optimized single-shot diffusion-weighted EPI sequence focusing on the thin olfactory tracts. To increase signal-to-noise ratio (SNR), two acquisitions were collected, using a standard brain protocol b value 1000 s/mm^2 . To reduce geometric warping, the TE was kept short by using maximum gradient strength/slew rate, parallel imaging, and partial Fourier encoding.

Fig. 2 Diffusion tensor imaging analysis of the anterior olfactory tracts of healthy controls (HC) and Parkinson's disease (PD) patients: (left panel) fractional anisotropy (FA) and (right panel) tract volume (TV)

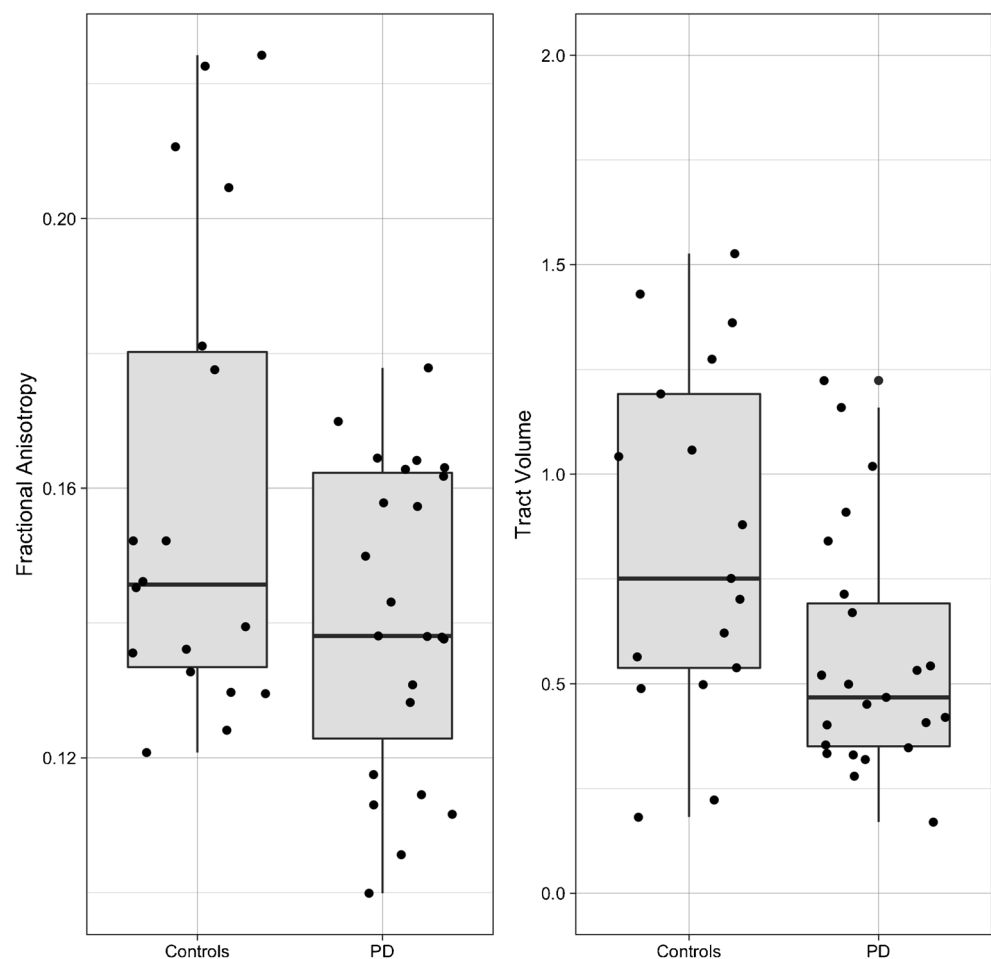
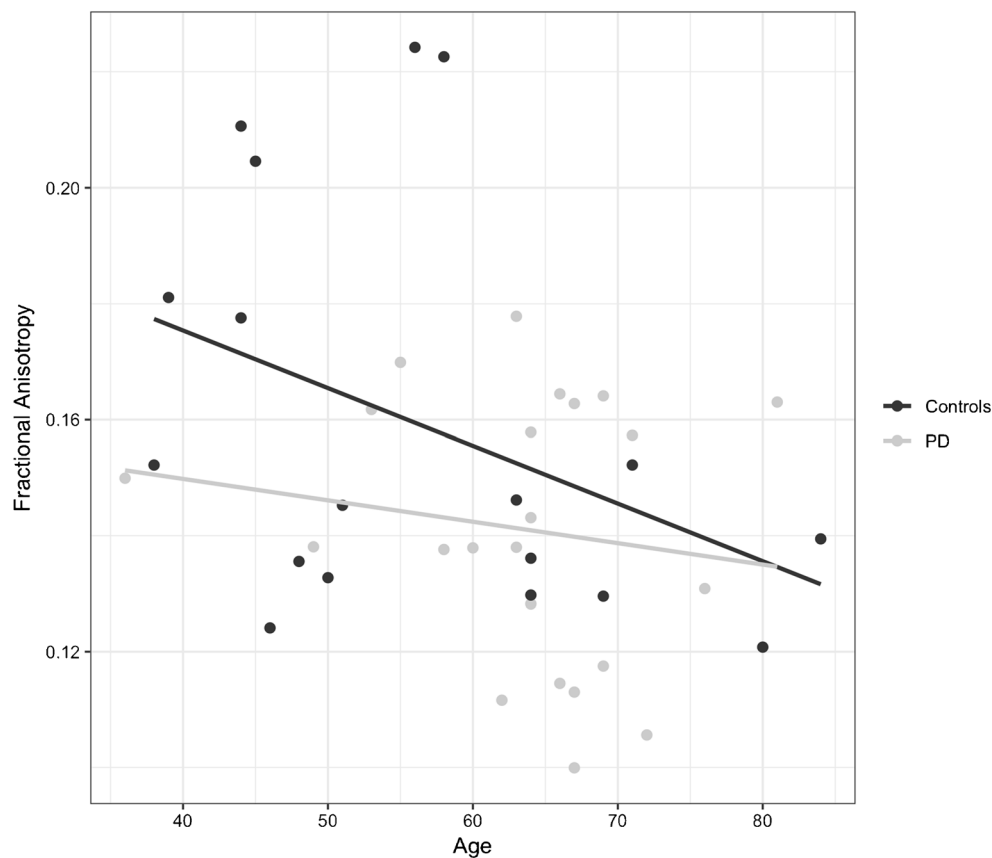


Fig. 3 Correlation between fractional anisotropy (FA) values and age in PD patients and in HC group. A significant correlation between FA and age, only for HC, was found ($r = -0.36$, $P < 0.05$, Spearman's rank correlation)



Unlike the only previously published study on DTI tractography [20], which failed to visualize the olfactory tracts in the single analyzed PD patient, we used a 3 T MRI scanner and achieved a higher SNR, and the voxel of our DTI acquisition was smaller, therein leading to a lower overall partial volume effect.

The most significant finding was the difference between the two group distributions for DTI values particularly FA and TV. This was most likely due to a disruption of fibers, which is in line with neuropathological observations which exhibited extensive extranigral changes for the PD patients.

Furthermore, significant correlations were found between FA values and age in the HC group. As in previous reports [24] in our cohort of patients, no correlation between severity of the motor dysfunction and DTI values of the olfactory tract was observed, suggesting that the time courses of developing motor impairments and the neuropathological processes within the anterior olfactory systems are divergent. So, our finding is in agreement with the Braak model of temporal degeneration in PD that hypothesizes α -synuclein pathology in both the olfactory bulbs and tracts occurring well before any nigral pathology. To this regard, the olfactory bulb has been proposed as an entry point for pathogens or

environmental insults, which can trigger the spread of pathological changes throughout the brain [31, 32]. Recently, the “prion” hypothesis has been proposed [33], which states that by spreading into the brain and acting as templates for endogenous proteins to form pathological aggregates, misfolded proteins resistant to degradation are responsible for disease [34]. Our findings, in line with this hypothesis and together with the anatomy of the olfactory system (bypassing the blood-brain barrier), suggest that a breakdown in the olfactory system might be the initiating clinical marker of the PD in progress. Moreover, additional research is needed to explore whether fiber tracking DTI changes in olfactory tracts are present in prodromal PD.

We recognize several limitations of our study. First, there were a low number of patients included in each group. Second, at our center, we did not have the availability of more than one expert tractographer, so an inter-rater agreement could not be provided. Third, the healthy controls, although accurately selected, were presumed to be normosmic and thus not tested by IOIT. Last, our cohorts were indistinguishable along two axes, namely, PD vs controls and hyposmic vs normosmic, making it impossible to reliably attribute change to one issue or another.

In conclusion, the result of our study demands that we further investigate to reveal the underlying mechanisms associated with hyposmia as seen in most PD patients.

Acknowledgments The Movement Disorders Center of the University of Perugia was supported by a grant from the New York University School of Medicine and the Marlene and Paolo Fresco Institute for Parkinson's and Movement Disorders, which was made possible with support from Marlene and Paolo Fresco.

Authors' contribution All authors have approved the final article.

Funding No funding was received for this study.

Compliance with ethical standard

Conflict of interest NT received a travel grant from Abbvie. PaC received research support from Bayer Schering, Biogen-Dompé, Boehringer Ingelheim, Eisai, Lundbeck, Merck-Serono, Novartis, Sanofi-Aventis, Sigma-Tau, and UCB Pharma. PN, AC, PE, SS, FPP, GC, PC, MF, RT, GG, VS, and LP declare that there are no disclosures to report.

Ethical approval The study was reviewed and approved by the local ethic committee.

Informed consent After a full explanation of the study, written informed consent was obtained from all participants according to the Declaration of Helsinki.

References

- Chaudhuri KR, Healy DG, Schapira AH (2006) Non-motor symptoms of Parkinson's disease: diagnosis and management. *Lancet Neurol* 5:235–245
- Hawkes CH, Del Tredici K, Braak H (2007) Parkinson's disease: a dual-hit hypothesis. *Neuropathol Appl Neurobiol* 33:599–614
- Braak H, Del Tredici K, Rüb U, de Vos RA, Jansen Steur EN, Braak E (2003) Staging of brain pathology related to sporadic Parkinson's disease. *Neurobiol Aging* 24:197–211
- Hawkes CH (2008) The prodromal phase of sporadic Parkinson's disease: does it exist and if so how long is it? *Mov Disord* 23:1799–1807
- Fullard ME, Morley JF, Duda JE (2017) Olfactory dysfunction as an early biomarker in Parkinson's disease. *Neurosci Bull* 33:515–525
- Postuma RB, Berg D (2016) Advances in markers of prodromal Parkinson disease. *Nat Rev Neurol* 12:622–634
- Hummel T, Witt M, Reichmann H, Welge-Luessen A, Haehner A (2009) Immunohistochemical, volumetric, and functional neuroimaging studies in patients with idiopathic Parkinson's disease. *J Neurol Sci* 289:119–122
- Silveira-Moriyama L, Holton JL, Kingsbury A, Ayling H, Petrie A, Sterlacci W, Poewe W, Maier H, Lees AJ, Revesz T (2009) Regional differences in the severity of Lewy body pathology across the olfactory cortex. *Neurosci Lett* 453:77–80
- Del Tredici K, Ru BU, De Vos RA, Bohl JR, Braak H (2002) Where does parkinson disease pathology begin in the brain? *J Neuropathol Exp Neurol* 61:413–426
- Politis M, Wu K, Molloy SG, Bain P, Chaudhuri KR, Piccini P (2010) Parkinson's disease symptoms: the patient's perspective. *Mov Disord* 25:1646–1651
- Brooks DJ, Tamasco N (2016) Imaging synucleinopathies. *Mov Disord* 31:814–829
- Su M, Wang S, Fang W, Zhu Y, Li R, Sheng K, Zou D, Han Y, Wang X, Cheng O (2015) Alterations in the limbic/paralimbic cortices of Parkinson's disease patients with hyposmia under resting-state functional MRI by regional homogeneity and functional connectivity analysis. *Parkinsonism Relat Disord* 21(7):698–703
- Scherfler C, Schocke MF, Seppi K, Esterhammer R, Brenneis C, Jaschke W, Wenning GK, Poewe W (2006) Voxel-wise analysis of diffusion weighted imaging reveals disruption of the olfactory tract in Parkinson's disease. *Brain* 129:538–542
- Zhang K, Yu C, Zhang Y, Wu X, Zhu C, Chan P, Li K (2011) Voxel-based analysis of diffusion tensor indices in the brain in patients with Parkinson's disease. *Eur J Radiol* 77:269–273
- Ibarretxe-Bilbao N, Junque C, Martí MJ, Valldeoriola F, Vendrell P, Bargallo N, Zarei M, Tolosa E (2010) Olfactory impairment in Parkinson's disease and white matter abnormalities in central olfactory areas: a voxel-based diffusion tensor imaging study. *Mov Disord* 25:1888–1894
- Basser PJ, Mattiello J, LeBihan D (1994) MR diffusion tensor spectroscopy and imaging. *Biophys J* 66:259–267
- Alexander AL, Lee JE, Lazar M, Field AS (2007) Diffusion tensor imaging of the brain. *Neurotherapeutics* 4:316–329
- Abhinav K, Yeh FC, Pathak S, Suski V, Lacomis D, Friedlander RM, Fernandez-Miranda JC (2014) Advanced diffusion MRI fiber tracking in neurosurgical and neurodegenerative disorders and neuroanatomical studies: a review. *Biochim Biophys Acta* 1842:2286–2297
- Schulte T, Sullivan EV, Müller-Oehring EM, Adalsteinsson E, Pfefferbaum A (2005) Corpus callosal microstructural integrity influences interhemispheric processing: a diffusion tensor imaging study. *Cereb Cortex* 15:1384–1392
- Skorpil M, Rolheiser T, Robertson H, Sundin A, Svenningsson P (2011) Diffusion tensor fiber tractography of the olfactory tract. *Magn Reson Imaging* 29:289–292
- Daniel SE, Lees AJ (1993) Parkinson's Disease Society Brain Bank, London: overview and research. *J Neural Transm Suppl* 39:165–172
- Maremmanni C, Rossi G, Tamasco N, Fattori B, Pieroni A, Ramat S, Napolitano A, Vanni P, Serra P, Piersanti P, Zanetti M, Coltelli M, Orsini M, Marconi R, Purcaro C, Rossi A, Calabresi P, Mecocci G (2012) The validity and reliability of the Italian Olfactory Identification Test (IOIT) in healthy subjects and in Parkinson's disease patients. *Parkinsonism Relat Disord* 18:788–793
- Ri D, Stern MB, Pfeiffer C, Gollomp SM, Hurtig HI (1992) Bilateral olfactory dysfunction in early stage treated and untreated idiopathic Parkinson's disease. *J Neurol Neurosurg Psychiatry* 55:128–142
- Scherfler C, Esterhammer R, Nocker M, Mahlknecht P, Stockner H, Warwitz B, Spielberger S, Pinter B, Donnemiller E, Decristoforo C, Virgolini I, Schocke M, Poewe W, Seppi K (2013) Correlation of dopaminergic terminal dysfunction and microstructural abnormalities of the basal ganglia and the olfactory tract in Parkinson's disease. *Brain* 136:3028–3037
- Oguz I, Farzinfar M, Matsui J, Budin F, Liu Z, Gerig G, Johnson HJ, Styner M (2014) DTIPrep: quality control of diffusion-weighted images. *Front Neuroinform* 8:4
- Wang R, Benner T, Sorensen AG et al (2007) Diffusion toolkit: a software package for diffusion imaging data processing and tractography. *Proc Intl Soc Mag Reson Med* 15:3720
- Atkinson-Clement C, Pinto S, Eusebio A, Coulon O (2017) Diffusion tensor imaging in Parkinson's disease: review and meta-analysis. *NeuroImage Clin* 16:98–110

28. Rolheiser TM, Fulton HG, Good KP, Fisk JD, McKelvey JR, Scherfler C, Khan NM, Leslie RA, Robertson HA (2011) Diffusion tensor imaging and olfactory identification testing in early-stage Parkinson's disease. *J Neurol* 258:1254–1260
29. Chen NK, Chou YH, Sundman M, Hickey P, Kasoff WS, Bernstein A, Trouard TP, Lin T, Rapcsak SZ, Sherman SJ, Weingarten CP (2018) Alteration of diffusion-tensor magnetic resonance imaging measures in brain regions involved in early stages of Parkinson's disease. *Brain Connect* 8:343–349
30. Nigro S, Riccelli R, Passamonti L, Arabia G, Morelli M, Nisticò R, Novellino F, Salsone M, Barbagallo G, Quattrone A (2016) Characterizing structural neural networks in de novo Parkinson disease patients using diffusion tensor imaging: altered structural brain network in drug-Naïve PD. *Hum Brain Mapp* 37:4500–4510
31. Dando SJ, Mackay-Sim A, Norton R, Currie BJ, St John JA, Ekberg JA, Batzloff M, Ulett GC, Beacham IR (2014) Pathogens penetrating the central nervous system: infection pathways and the cellular and molecular mechanisms of invasion. *Clin Microbiol Rev* 27:691–726
32. Doty RL (2008) The olfactory vector hypothesis of neurodegenerative disease: is it viable? *Ann Neurol* 63:7–15
33. Rey NL, Wesson DW, Brundin P (2018) The olfactory bulb as the entry site for prion-like propagation in neurodegenerative diseases. *Neurobiol Dis* 109:226–248
34. Aguzzi A, Baumann F, Bremer J (2008) The Prion's elusive reason for being. *Annu Rev Neurosci* 31:439–477

Publisher's note Springer Nature remains neutral with regard to jurisdictional claims in published maps and institutional affiliations.